The Astrophysical Journal, 616:L131–L134, 2004 December 1

THE DOUBLE PULSAR SYSTEM J0737−3039: MODULATION OF A BY B AT ECLIPSE

M. A. McLaughlin,[1] A. G. Lyne,[1] D. R. Lorimer,[1] A. Possenti,[2] R. N. Manchester,[3] F. Camilo,[4] I. H. Stairs,[5] M. Kramer,[1] M. Burgay,[2] N. D'Amico,[6] P. C. C. Freire,[7] B. C. Joshi,[8] and N. D. R. Bhat[9]

Received 2004 August 16; accepted 2004 October 18; published 2004 October 27

ABSTRACT

We have investigated the eclipse of the 23 ms pulsar, PSR J0737−3039A, by its 2.8 s companion PSR J0737−3039B in the recently discovered double pulsar system using data taken with the Green Bank Telescope at 820 MHz. We find that the pulsed flux density at eclipse is strongly modulated with the periodicity of the 2.8 s pulsar. The eclipse occurs earlier and is deeper at those rotational phases of B when its magnetic axis is aligned with the line of sight than at phases when its magnetic axis is at right angles to the line of sight. This is consistent with the eclipse of A being due to synchrotron absorption by the shock-heated plasma surrounding B, the asymmetry arising from the higher plasma densities expected in the B magnetosphere's polar cusps.

Subject headings: binaries: general — pulsars: general — pulsars: individual (PSR J0737−3039A, PSR J0737−3039B)

Online material: color figure

1. INTRODUCTION

The two pulsars in the recently discovered double pulsar binary system, J0737−3039A and J0737−3039B (hereafter simply A and B), have periods of $P_A = 23$ ms and $P_B = 2.8$ s. They are in a 2.4 hr mildly eccentric orbit that we view nearly edge-on, with an inclination angle of 87° ± 3° (Burgay et al. 2003; Lyne et al. 2004). The phenomenology exhibited by this system is extremely rich. The flux density of the B pulsar varies dramatically and systematically around the orbit (Lyne et al. 2004; Ramachandran et al. 2004; McLaughlin et al. 2004), indicating significant interaction between the two pulsars. While the flux density of the A pulsar is constant for most of the orbit, for ~30 s around its superior conjunction, A is eclipsed by the magnetosphere of B (Lyne et al. 2004). This eclipse is asymmetric, with the flux density of A decreasing more slowly on ingress than it increases on egress. The duration of the eclipse is mildly dependent on radio frequency, with eclipses lasting longer at lower frequencies (Kaspi et al. 2004).

Theoretical models by Arons et al. (2004) and Lyutikov (2004) explain these eclipse properties in the context of synchrotron absorption of A's radio emission by the shock-heated plasma surrounding and containing B's magnetosphere. Because B's magnetosphere will respond differently to the pressure of the relativistic wind of A at different rotational phases of B, one prediction of these models is that the density of absorbing plasma, and hence the properties of A's eclipse, will depend on the rotational phase of B. In their early analysis of the exploratory observations performed at the 100 m Green Bank Telescope (GBT) in 2003 December and 2004 January, Kaspi et al. (2004) found no evidence for modulation of the eclipse properties with B's rotational phase. We have analyzed this publicly available data set and, in this Letter, show that the eclipse properties of A are in fact strongly dependent on the rotational phase of B.

2. OBSERVATIONS AND ANALYSIS

The double pulsar system J0737–3039 was observed at the GBT in 2003 December and 2004 January using receivers centered at 427, 820, and 1400 MHz. The 5 hr 820 MHz observation discussed here was acquired with the GBT Spectrometer SPIGOT card with a sampling time of 40.96 μs and 1024 synthesized frequency channels covering a 50 MHz bandwidth. For more details of the observations and data acquisition system, see Ransom et al. (2004) and references therein.

The data were dedispersed and folded using freely available software tools (Lorimer 2001), assuming the nominal dispersion measure of 48.9 cm^{-3} pc (Burgay et al. 2003) and using ephemerides for A and B from Lyne et al. (2004). We folded the data with 512 phase bins and, for each A pulse, calculated the mean pulsed flux density in two on-pulse phase windows centered on the two pulse components (Burgay et al. 2003). From these, we subtracted the baseline level calculated from two off-pulse windows. The on- and off-pulse regions contained 95 and 320 phase bins, respectively. For each orbit, we created a light curve of A's pulsed flux density with time by averaging every 12 pulses, for an effective time resolution of ~0.27 s. Orbital phases were calculated using the modified Julian dates of pulse arrival at the solar system barycenter and the pulsar ephemeris. Analysis of these light curves reveals that for the majority of the orbit, the pulsed flux density of A is constant within measurement uncertainties, exhibiting no obvious orbital phase-dependent variations. However, close to superior conjunction (i.e., orbital phase 90°, where orbital phase is defined as the longitude from the ascending node) the pulsed flux density of A varies dramatically.

Figure 1 shows the light curves of A for all three eclipses

[1] Jodrell Bank Observatory, University of Manchester, Macclesfield, Cheshire SK11 9DL, UK.
[2] INAF–Osservatorio Astronomico di Cagliari, Locanda Poggio dei Pini, Strada 54, 09012 Capoterra, Italy.
[3] Australia Telescope National Facility, CSIRO, P.O. Box 76, Epping NSW 1710, Australia.
[4] Columbia Astrophysics Laboratory, Columbia University, 550 West 120th Street, New York, NY 10027.
[5] Department of Physics and Astronomy, University of British Columbia, 6224 Agricultural Road, Vancouver, BC V6T 1Z1, Canada.
[6] Università degli Studi di Cagliari, Dipartimento di Fisica, SP Monserrato-Sestu km 0.7, 09042 Monserrato, Italy.
[7] National Astronomy and Ionosphere Center, Arecibo Observatory, HC03 Box 53995, PR 00612.
[8] National Center for Astrophysics, P.O. Bag 3, Ganeshkhind, Pune 411007, India.
[9] Massachusetts Institute of Technology, Haystack Observatory, Westford, MA 01886.

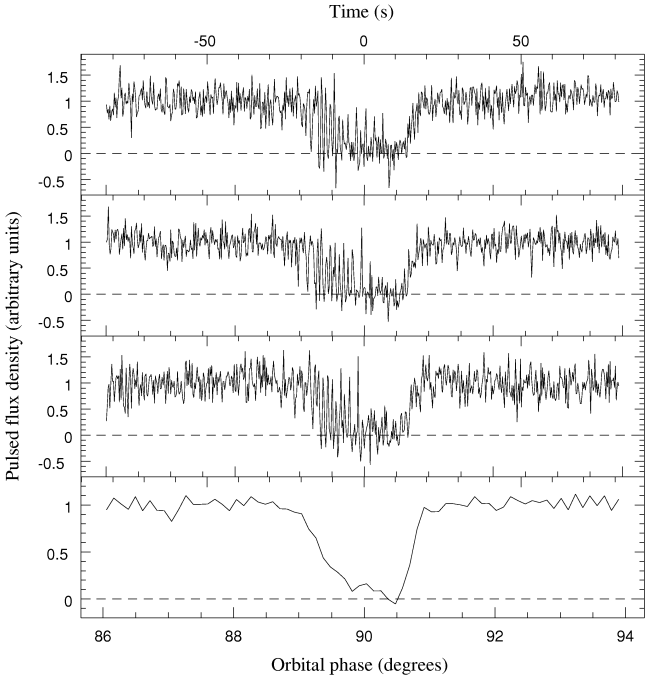

FIG. 1.—Pulsed flux density of A vs. time (with respect to superior conjunction) and orbital phase for the three eclipses in the 820 MHz observation (*top three panels*) and all three eclipses summed (*bottom panel*). In the individual eclipse light curves, every 12 pulses have been averaged for an effective time resolution of ~0.27 s. Every 100 pulses have been averaged to create the lower composite light curve for an effective time resolution of ~2.3 s. Pulsed flux densities have been normalized such that the preeclipse average flux density is unity.

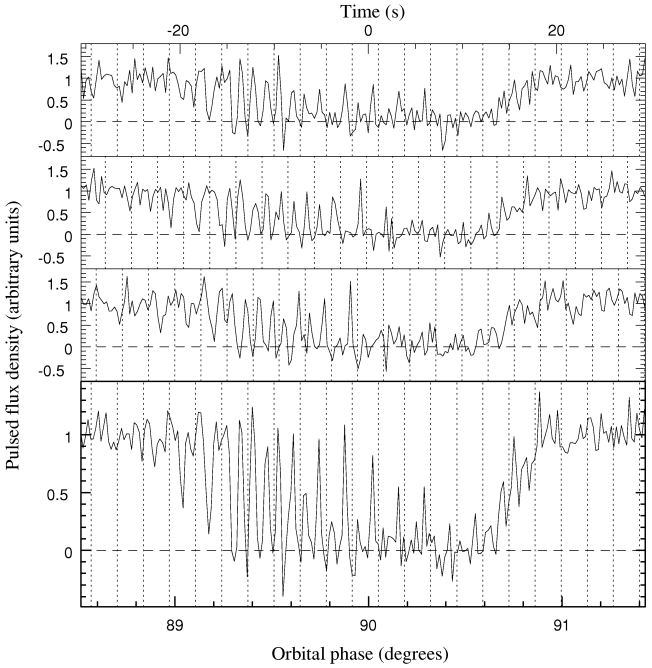

FIG. 2.—As in Fig. 1, the top three panels show the light curves for the three individual eclipses but covering a narrower range of orbital phase. The vertical dashed lines indicate the measured arrival times of the pulses of B. The bottom panel shows the light curve averaged over all three eclipses of A, with the second and third eclipses shifted by less than $\pm P_B/2$ so that the B pulses arrive at the same phase as during the first eclipse. Because limited signal-to-noise ratio prohibits us from summing over a smaller number of pulses, it is likely that the true structure of the flux density peaks and dips is finer than it appears in this figure.

included in the 820 MHz observation. In the bottom panel, we also show a composite light curve, averaged over all three eclipses and over 100 A pulses, for an effective time resolution of ~2.3 s. Our measurements of the eclipse duration and of ingress and egress shapes from this composite light curve are consistent with the results of Kaspi et al. (2004), who averaged data in 2 s intervals. They calculated an eclipse duration (defined by the FWHM of the light curve) of 27 s, which was used to place a limit of 18,600 km on the size of the eclipsing region. They also found that eclipse ingress takes roughly 4 times longer than egress and that the eclipse duration is frequency-dependent, lasting longer at lower frequencies.

Inspection of the top three panels of Figure 1 shows that the rise and fall of the flux density during eclipse is not monotonic. In fact, up until orbital phases approaching 90°, the light curves of A show amplitude peaks consistent with preeclipse levels. Figure 2 shows an expanded view of Figure 1 covering a smaller range of orbital phases centered on the eclipse. On this plot, we also indicate the measured barycentric arrival times of the pulses of the 2.8 s pulsar B. This demonstrates clearly that the pulsed flux density of A is modulated in synchronism with $0.5P_B$. In all three eclipses, we see negative dips in pulsed flux density occurring first at a time about $0.5P_B$ out of phase with the B pulses and later also at a time in phase with the B pulses. In order to determine more sensitively how the flux density of A depends on the rotational phase of B, we shifted the light curves of the second and third eclipses by up to $\pm 0.5P_B$ so that the phases of the B pulses were identical to those of the first eclipse. We then summed the light curves of all three eclipses to create the bottom panel of Figure 2. Dividing each 2.8 s window of B's rotational phase into four equal regions, we can calculate an average light curve for each region, as shown in Figure 3. The light curves for each of the B pulse phase windows vary smoothly.

Eclipse durations range from 20 to 34 s for the four B phase windows, calculated, as in Kaspi et al. (2004), to be the FWHM of the eclipse. Ingress occurs first at B phase 0.5 and then at 0.0, when, assuming that B is an orthogonal rotator, the magnetic axis of B is aligned with the line of sight to A. It occurs later and more gradually for the other two phase windows centered on phases 0.25 and 0.75, when the magnetic axis of B is at right angles to the line of sight. The orbital phases of egress are similar for all B pulse phases. For light curves at B phases centered on 0.0 and 0.5, the eclipses are essentially symmetric, with a minimum beginning at orbital phases near 89°.4 and ending at orbital phases near 90°.6. The light curves for B phases centered on 0.25 and 0.75 are less symmetric, with the flux density minimum occurring briefly, around orbital phases 90°.2–90°.5. Only at around orbital phase 90°.5 is the flux density of all phases of B consistent with being zero.

It is important to recognize that the features we see in the 820 MHz data cannot be due to confusion with the single pulses of B (e.g., McLaughlin et al. 2004), since the pulsed features seen in Figure 2 are not in phase with the radio pulses of B, and, in addition, the latter, which have a width of ~50 ms, would be removed by the on-pulse/off-pulse subtraction procedure used to determine A's flux density.

3. DISCUSSION

Our analysis of these data differs from that of Kaspi et al. (2004) in one significant respect. While Kaspi et al. (2004) calculated light curves with 2 s time resolution, we have integrated over only 12 A pulses, affording us ~7 times better

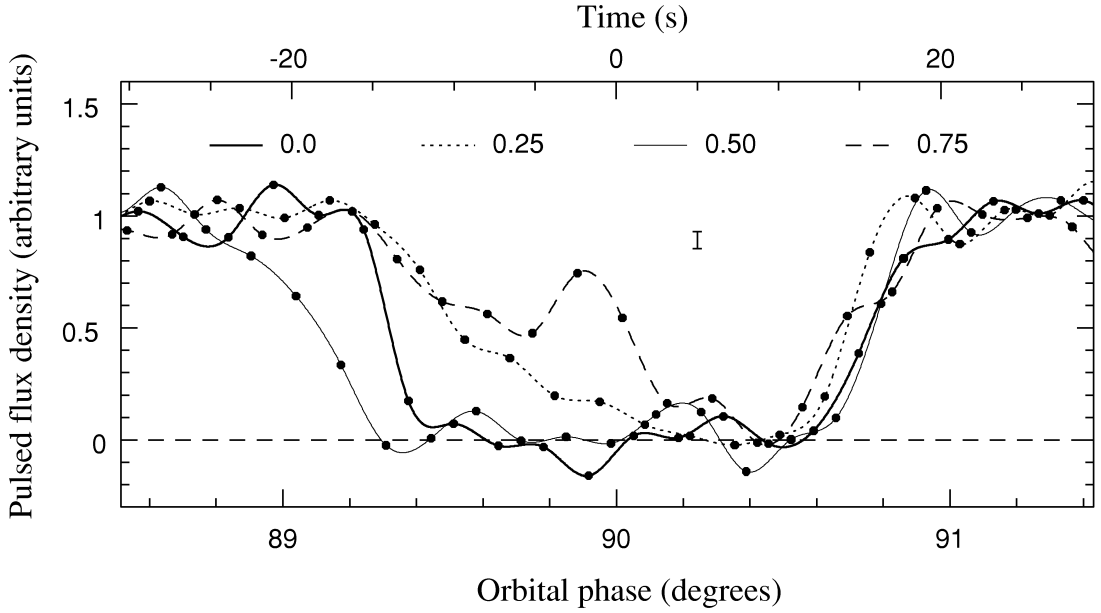

FIG. 3.—Averaged light curves for four regions of B pulse phase, with a smooth curve calculated with a spline fitting procedure drawn through the individual flux density measurements. The four regions are centered on pulse phases 0.0, 0.25, 0.50, and 0.75 with, for example, the curve for 0.0 covering the 0.25 of pulse phase centered on B's radio pulse. Fig. 4 shows the geometry of the system at this B pulse phase. The vertical bar indicates the typical $\pm 1\ \sigma$ measurement error in each flux density. [*See the electronic edition of the Journal for a color version of this figure.*]

time resolution. Kaspi et al. (2004) did detect some emission from A on short timescales during the eclipse, but their 2 s integration time was not sufficient to detect the B modulation. We have shown that the eclipse duration varies considerably with B phase and, hence, that the properties of the occulting medium are in fact different in different regions of B's magnetosphere.

The observed eclipse phenomenology can be understood in the context of a model invoking synchrotron absorption of the radio emission from A in a magnetosheath surrounding B's rotating magnetosphere (Arons et al. 2004; Lyutikov 2004). Much of the rotational energy of the faster spinning A pulsar is emitted in the form of a relativistic magnetized wind composed primarily of electron-positron pairs. The rotational energy loss rate of A (6×10^{33} ergs s^{-1}) is ~3600 times greater than that of the slower B pulsar. Because the dynamic pressure of A's wind is balanced against B's magnetic pressure only at a point well inside the light cylinder of B, A's wind confines the B magnetosphere on the side facing A, with a long magnetospheric tail extending behind B. The collision of A's wind with the magnetosphere of B leads to the formation of a bow shock consisting of hot magnetized plasma. This plasma will surround the cometary-shaped magnetosphere of B, creating what Arons et al. (2004) call a "magnetosheath." In Figure 4, we show a schematic of the interaction of A's relativistic wind with B's magnetosphere. The rotation of B inside the magnetosheath is expected to modulate the shape of the sheath and to produce cusps within it, leading to higher plasma densities in the cusps. Note that the plasma will not reach all the way to the polar caps of B but is confined at the "magnetopause," where the plasma pressure equals the magnetic pressure. An excellent description of the shape of the magnetosphere and of the polar cusps is given in Arons & Lea (1976).

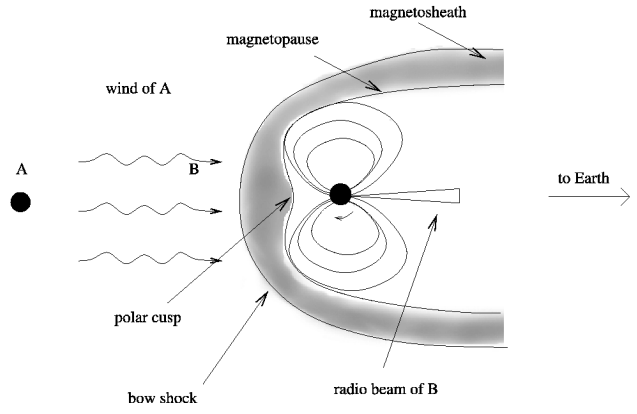

FIG. 4.—Cartoon (not to scale) showing the interaction between the relativistic wind of A and the magnetosphere of B when the radio beam of B is pointing toward the Earth (i.e., pulse phase 0.0). For a more detailed picture of this interaction, see Fig. 2 of Arons et al. (2004).

As already discussed qualitatively by Kaspi et al. (2004) and quantitatively by Arons et al. (2004) and Lyutikov (2004), synchrotron absorption in such a magnetosheath can explain many of the properties of the A eclipse, including the sharp edge and the mild frequency dependence. If B is rotating prograde to the orbital velocity, it can also explain the asymmetry between eclipse ingress and egress. The observed changes in eclipse properties with B pulse phase give further support to the model. The pulses from A are first absorbed at the two B pulse phases (i.e., 0.0 and 0.5) at which the magnetic axis of B is aligned with the line of sight to A. This can be attributed to the higher density of absorbing plasma in B's polar cusps. Note that the pulses at B pulse phase 0.50 (i.e., when the radio-bright pole is pointed toward A) are absorbed before those at B pulse phase 0.0. When the line of sight to A is at a right angle to B's magnetic axis, the pulses of A travel through regions of higher plasma density later in the orbit and start fading closer to superior conjunction, where the opacity of the magnetosheath tail could also become predominant. As shown in Figure 3, the ingress phase and eclipse duration for these two B phases (i.e., 0.25 and 0.75) differ, with absorption hap-

pening later at phase 0.75. This may be due to the rotationally induced asymmetry predicted by Arons et al. (2004).

The above discussion and the simulations of Arons et al. (2004) assume that B is an orthogonal rotator. As Demorest et al. (2004) and Arons et al. (2004) discuss, it is quite likely that this is the case, as the wind torque from A should have aligned B's rotation axis with the orbital angular momentum. Furthermore, it is very difficult to explain the similarity between the light curves at B pulse phases 0.0 and 0.5 and phases 0.25 and 0.75 if B is not nearly orthogonal.

From the measured eclipse durations, it is clear that the size of the eclipsing region is much smaller than the light cylinder of B. However, because the plasma density varies greatly depending on the rotational phase of B, determining the extent and density of the eclipsing region is not trivial and will require detailed modeling of the plasma density variations within B's magnetosphere. As a result of the effects of relativistic periastron advance and geodetic precession, the durations and morphologies of the eclipse and their dependence on the B rotational phase should change significantly with time. Forthcoming observations will allow us to sensitively probe the dynamics of the wind/magnetosphere interaction and of the geometry of the system. These observations, at multiple frequencies, will also allow us to test the hypothesis of Arons et al. (2004) that there should be no eclipse at frequencies above 5 GHz, already supported by the measurements of Kaspi et al. (2004).

Because pulsars emit a large portion of their spin-down energy in the form of a relativistic wind, understanding these winds is crucial for forming a complete picture of the pulsar energy budget. However, because the winds cannot be directly observed, progress in this field has been limited to studies of pulsar wind nebulae and bow shocks. If the eclipses of A are indeed caused by synchrotron absorption in B's magnetosheath, both Arons et al. (2004) and Lyutikov (2004) reach the very interesting conclusion that the density of A's wind must be at least 4 orders of magnitude greater than is expected given currently accepted models of pair creation. The Arons et al. (2004) model also implies a very low wind magnetization. However, in our Letter describing the drifting features observed in the single pulses of B (McLaughlin et al. 2004), we concluded that most of the spin-down energy is carried by the Poynting flux rather than by energetic particles. Clearly, self-consistent models that can explain both of these phenomena are needed. The rich phenomenology offered by the double pulsar system will offer us new ways to explore the physics of these winds on much smaller scales than has been possible with other systems. Eclipse measurements of the double pulsar system also may be important for constraining pulsar pair creation scenarios.

We thank A. Spitkovsky for a very useful discussion that motivated us to look for this effect and D. Melrose, F. Graham Smith, and J. Arons for helpful discussions. We thank the National Radio Astronomy Observatory for making these observations publicly available. The National Radio Astronomy Observatory is a facility of the National Science Foundation operated under cooperative agreement by Associated Universities, Inc. I. H. S. holds an NSERC UFA and is supported by a Discovery Grant. D. R. L. is a University Research Fellow funded by the Royal Society. N. D., A. P., and M. B. received support from the Italian Ministry of University and Research under the national program Cofin 2003.

REFERENCES

Arons, J., Backer, D. C., Spitkovsky, A., & Kaspi, V. M. 2004, in Binary Radio Pulsars, ed. F. Rasio & I. Stairs (San Francisco: ASP), in press (astro-ph/0404159)
Arons, J., & Lea, S. M. 1976, ApJ, 207, 914
Burgay, M., et al. 2003, Nature, 426, 531
Demorest, P., Ramachandran, R., Backer, D. C., Ransom, S. M., Kaspi, V., Arons, J., & Spitkovsky, A. 2004, ApJ, 615, L137
Kaspi, V. M., Ransom, S. M., Backer, D. C., Ramachandran, R., Demorest, P., Arons, J., & Spitkovsky, A. 2004, ApJ, 613, L137
Lorimer, D. R. 2001, Arecibo Tech. Memo 2001-01, http://www.jb.man.ac.uk/~drl/sigproc
Lyne, A. G., et al. 2004, Science, 303, 1153
Lyutikov, M. 2004, MNRAS, 353, 1095
McLaughlin, M. A., et al. 2004, ApJ, 613, L57
Ramachandran, R., Backer, D. C., Demorest, P., Ransom, S. M., & Kaspi, V. M. 2004, ApJ, in press (astro-ph/0404392)
Ransom, S. M., et al. 2004, ApJ, 609, L71